Journal of Geriatric Cardiology (2019) 16: 855–871

Research Article · Open Access ·

Hypoxia promotes pulmonary vascular remodeling via HIF-1α to regulate mitochondrial dynamics

Xi CHEN[1,2], Jia-Mei YAO[1,3,4], Xia FANG[2,3], Cui ZHANG[1,3], Yu-Shu YANG[1,3], Cheng-Ping HU[1,2], Qiong CHEN[1,3,4], Guang-Wei ZHONG[1,3,4,#]

[1]*National Center for Clinical Medicine for Geriatric Diseases, Xiangya Hospital, Central South University, Changsha, China*
[2]*Department of Respiratory Medicine, Xiangya Hospital, Central South University, Changsha, China*
[3]*Department of Geriatrics, Xiangya Hospital, Central South University, Changsha, China*
[4]*International Medical Center, Xiangya Hospital, Central South University, Changsha, China*

Abstract

Background Increasing research suggests that mitochondrial defect plays a major role in pulmonary hypertension (PH) pathogenesis. Mitochondrial dynamics and quality control have a central role in the maintenance of the cell proliferation and apoptosis balance. However, the molecular mechanism underlying of this balance is still unknown. **Methods** To clarify the biological effects of hypoxic air exposure and hypoxia-inducible factor-1α (HIF-1α) on pulmonary arterial smooth muscle cell (PASMC) and pulmonary arterial hypertension rats, the cells were cultured in a hypoxic chamber under oxygen concentrations. Cell viability, reactive oxygen species level, cell death, mitochondrial morphology, mitochondrial membrane potential, mitochondrial function and mitochondrial biosynthesis, as well as fission-and fusion-related proteins, were measured under hypoxic conditions. In addition, rats were maintained under hypoxic conditions, and the right ventricular systolic pressure, right ventricular hypertrophy index and right ventricular weight/body weight ratio were examined and recorded. Further, we assessed the role of HIF-1α in the development and progression of PH using HIF-1α gene knockdown using small interfering RNA transfection. Mdivi-1 treatment was performed before hypoxia to inhibit dynamin-related protein 1 (Drp1). **Results** We found that HIF-1α expression was increased during hypoxia, which was crucial for hypoxia-induced mitochondrial dysfunction and hypoxia-stimulated PASMCs proliferation and apoptosis. We also found that targeting mitochondrial fission Drp1 by mitochondrial division inhibitor Mdivi-1 was effective in PH model rats. The results showed that mitochondrial dynamics were involved in the pulmonary vascular remodeling under hypoxia *in vivo* and *in vitro*. Furthermore, HIF-1α also modulated mitochondrial dynamics in pulmonary vascular remodeling under hypoxia through directly regulating the expression of Drp1. **Conclusions** In conclusion, our data suggests that abnormal mitochondrial dynamics could be a marker for the early diagnosis of PH and monitoring disease progression. Further research is needed to study the signaling pathways that govern mitochondrial fission/fusion in PH.

J Geriatr Cardiol 2019; 16: 855–871. doi:10.11909/j.issn.1671-5411.2019.12.003

Keywords: Dynamin-related protein 1; Hypoxia; Hypoxia-inducible factor-1α; Mitochondrial dynamics; Pulmonary vascular remodeling

1 Introduction

Pulmonary hypertension (PH) is a pulmonary vascular remodeling disease that is characterized by a continuous and notable elevation of pulmonary arterial pressure (PAP) and pulmonary vascular resistance, which results in heart failure and death.[1] Although the pathogenesis of PH is a complex, multifactorial disease with largely unknown etiology, it has been abundantly documented that aberrant proliferation and apoptosis of pulmonary arterial smooth muscle cells (PASMCs) in the medial layer of pulmonary arteries are key pathological processes in the development of PH. However, the underlying mechanism remains a source of controversy.[2] Mitochondria are involved in a variety of cellular functions, including adenosine triphosphate (ATP) production, amino acid and lipid biogenesis, catabolism, signaling, and apoptosis.[3] Mitochondria are highly dynamic organelles whose location, size, and distribution are controlled by a family of proteins that modulate mitochondrial fusion and fission.[4] Optic atrophy 1 (OPA1), mitofusin 1 (Mfn1), and mitofusin 2 (Mfn2) are three fusion-related proteins. In addition, hypoxia to inhibit dynamin-related protein 1 (Drp1)

[#]**Correspondence to:** Guang-Wei ZHONG, Department of Geriatrics, Xiangya Hospital, Central South University, Changsha, China. E-mail: zgw7512@sina.com
Received: June 5, 2019 **Revised:** August 25, 2019
Accepted: September 24, 2019 **Published online:** December 28, 2019

and fission 1 (Fis1) are two molecules responsible for mitochondrial fission.[5] In recent decades, many researchers have found that mitochondria and PH not only share a similarly poor prognosis, but also a major pathophysiologic mechanism, including cell proliferation and abnormal metabolic pathway that constitutes the mitochondria dynamic.[6–8] This suggests that the mitochondria dynamic may play an essential role in cell proliferation related to the vascular remodeling process of PH. However, it remains unclear whether the mitochondria dynamic is involved in PASMCs proliferation and apoptosis.

PH can be caused by chronic hypoxia-induced pulmonary vasoconstriction and reconstruction; however, the exact mechanism is unclear. The increased expression of hypoxia-inducible factor-1α (HIF-1α) was found in the lung tissue of patients and animals with PH.[9,10] HIF-1α is a master transcriptional regulator that responds to a hypoxic environment and induces the transcription of genes, including vascular endothelial growth factor, glucose transporter 1, and pyruvate dehydrogenase kinase 1, which promote PASMCs proliferation and migration.[11,12] Under hypoxia, the mitochondrial electron transport chain regulates the production of mitochondrial-derived oxygen-free radicals and reactive oxygen species (ROS).[13] Of the ROS molecules involved in this process, H_2O_2 is a permeable biofactor that can activate the transcription factor and lower oxygen-induced factor HIF-1α,[14] resulting in the opening and activation of the mitochondrial ATP-sensitive potassium channel of PASMCs.[15] This results in a positive feedback on the ROS level and the expression of HIF-1α,[16] which promotes the proliferation of PASMCs and inhibits their apoptosis,[17] and taking part in the remodeling process of chronic hypoxic pulmonary blood vessels. Cyclin B1/cyclin-dependent kinase 1-dependent phosphorylation of Drp1 at serine 616-mediated mitochondrial fission leads to increased proliferation in human PH PASMCs.[18] Studies have shown that HIF-1α inhibitors and mitochondria dynamic inhibitors attenuate hypoxia-induced PASMCs proliferation and apoptosis.[19,20] To date, many investigators have focused on mitochondrial homeostasis, including fission/fusion changes that occur in human diseases.[21] However, the full spectrum of pathophysiological mechanisms of mitochondria that result in chronic hypoxic PH have yet to be determined. In addition, the relative importance and potential relationship between hypoxia and mitochondrial dynamics have not been completely explored.

Thus, we hypothesized that hypoxia promotes pulmonary vascular remodeling via HIF-1α to regulate mitochondrial dynamics through Drp1 and promote PASMC proliferation and apoptosis. In this study, we investigated the effect of HIF-1α in the mitochondrial dynamics and PASMCs proliferation and apoptosis *in vitro* and *in vivo*. Our data indicated that HIF-1α resulted in an increase of mitochondrial fission in the proliferation and apoptosis state of PASMCs, and the mechanism involved the activation of downstream HIF-1α/Drp1 signaling pathways.

2 Materials and methods

2.1 Reagents and antibodies

Antibody against OPA1 was obtained from BD Biosciences (Bedford, MA) (catalog number 612606). Antibodies against α-smooth muscle actin (α-SMA), Mfn1, Mfn2, Drp1, and Fis1 were purchased from Santa Cruz Biotechnology, Inc. (Santa Cruz, USA). Antibodies against HIF-1α and β-actin were purchased from Cell Signaling Technology, Inc. (CST, Boston, USA). Antibodies against Caspase 3 and proliferating cell nuclear antigen (PCNA) were obtained from Boster (Wuhan, China). The construction of recombinant adenovirus expressing the HIF-1α and the Ad-HIF-1α was done by Shanghai Genechem Co., LTD, China. The drug mitochondrial division inhibitor, Mdivi-1 (6338967-87-6), was purchased from Sigma-Aldrich Inc. (CST, Boston, USA). Mitochondrial respiratory chain complex V (ATP synthase) quantitative detection kit was purchased from Suzhou Keming Biotechnology Co., Ltd., China. Cytochrome C Oxidase Activity Assay Kit was purchased from Nanjing Construction Biology Co., Ltd., China.

2.2 Preparation of AAV2-HIF-1α-shRNA

A U6 promoter-driven short hairpin RNA (shRNA) expression system was established in an AAV2 vector. Green fluorescent protein (GFP) expression was separately controlled by a CMV promoter as a marker for transduction efficiency. HIF-1α shRNA was designed based on the small interfering RNA (siRNA) sequence (GenBank Acc. NM_001530.3) using an siRNA design tool (Biomiao, Beijing, China) and was screened according to the guidelines reported by Fang X, *et al*.[22] Four selected siRNA target sequences were inserted between the KpnI and EcoRI sites in a U6-CMV-EGFP/AAV vector, and an optimal HIF-1α target (sequence: 5'-GCTGGAGACACAATCATAT-3') was selected. A recombinant adenovirus carrying a siRNA sequence targeting the EGFP reporter gene (sequence: 5'-CACCGTTCTCGACGTGTCACGTCAGAGATTACTGACACGTTCGAGAATTTTG-3') was included as a control. Both the adenovirus- HIF-1α-shRNA and negative control vectors contained the sequence encoding GFP. All constructs were verified by DNA sequencing, all viral vectors were generated by tripleplasmid cotransfection of human

293 cells, and recombinant virions were column purified as previously described.[23] Next, viral titers were determined using quantitative polymerase chain reaction (PCR). The resulting AAV2-HIF-1α-shRNA titer was determined to be 7.43×10^{11} pfu/mL, and the AAV2-GFP titer was 5.96×10^{11} pfu/mL.

2.3 Animal

Male Sprague-Dawley (SD) rats (weighing: 150–200 g) obtained from the Laboratory Animal Center at the Central South university (Changsha, China) were used for the hypoxia-induced PH model as previously described.[24] Briefly, the animals were randomly and equally divided into two groups: normoxic control group (21% O_2) and a hypoxic group (10% ± 0.5% O_2). All live animals were handled in accordance with National Institutes of Health Guide for the Care and Use of laboratory Animal and approved by the Ethics Committee of the Xiangya hospital, Central South University.

HIF-1α knockdown experiment was performed to evaluate the prevention and reversal effect of HIF-1α inhibition, the rats were randomly assigned to the following groups: the normal group (n = 6), model group (n = 6), control group (n = 6), shRNA group (n = 6) and Mdivi-1 group (n = 6). The control group received tail vein injection of AAV-GFP-shRNA, while the shRNA group received tail vein injection of AAV-shRNA-HIF-1α (100 μl, 1×10^{11} pfu) at two weeks prior or two weeks after hypoxia. The Mdivi-1 group received intraperitoneal injection of Mdivi-1 solution (50 mg/kg, dissolved by dimethyl sulfoxide) for half an hour before hypoxia. All animals were sacrificed at four weeks after hypoxia. Hemodynamic, morphologic, and biochemical assessments were performed.

2.4 Cell culture and transfection

PASMCs were isolated from the pulmonary arteries of 15-week-old male SD rats using our laboratory's previously described method.[25] The cells were cultured at 37 °C under 5% CO_2 in Dulbecco's modified Eagle's medium containing 20% fetal bovine serum. PASMCs were identified by immunohistochemical staining and immunofluorescence staining using an antibody against smooth muscle α-SMA. For hypoxia (3% O_2) experiments, cells were put into gas-tight modular incubator chambers (Thermo, Carlsbad, CA, USA), which were infused with a gas mixture containing 5% CO_2 and 92% N_2 for 24 hours. Normal incubators with 21% O_2 were used for the normoxic cultures.

PASMCs (80% confluent) were treated according to the manufacturer's instructions with HIF-1α siRNAs (mouse, Santa Cruz Biotechnology, USA) for 72 hours to inhibit HIF-1α expression. Transfection of PASMCs by siRNA was achieved using Lipofectamine 2000 (Invitrogen). In brief, HIF-1α siRNA and control siRNA with the transfection reagent were incubated for 20 minutes, to form complexes, which then were added to plates containing cells and medium. The cells were incubated at 37 °C in a CO_2 incubator for further analysis.

2.5 Hemodynamic measurements

On the end of fourth week, all rats were narcotized with 3% sodium pentobarbital (40 mg/kg). The data of right ventricular systolic pressure (RVSP) and mean PAP (mPAP) were kept as records under the same factors, as previously described.[26] Hemodynamic indexes were surveyed by a pressure pickup and a polygraph system (RM6000, Nihon Kohden, Tokyo, Japan) for recording. The Fulton index [the ratio of RV weight to left ventricle þ septum weight, RV/(LV + S)] or RV weight relative to the animal's body weight (RV/BW) was determined as a measurement for RV hypertrophy.

2.6 Pulmonary arterial morphometry

We performed histopathological observations as previously described.[26] We used 4% paraform and sterile physiological saline to exsanguinate the rats. We then detached the right inferior lobe of the lungs and fixed them with 4% paraform. After embedding in paraffin, the lungs were sectioned to produce 5-μm-thick sections which were stained with hematoxylin and eosin (H & E) and Masson. Twelve pulmonary arteries per rat were investigated using a BX51 (Olympus, Tokyo, Japan) system in six rats/group. Percentage medial muscle thickness was measured to reflect pulmonary remodeling, which was calculated as follows: pulmonary wall thickness (%) = (external diameter-internal diameter)/external diameter × 100%, as previously described.

2.7 Transmission electron microscopy

According to the conventional transmission electron microscopy sample preparation method.[25] The slices were then postfixed in a 1% osmium-tetroxide phosphate-buffered saline (PBS) for two hours, and subsequently rinsed, dehydrated, saturated, and embedded in EPON812 resin. Then, ultrathin slices were cut on an ultramicrotome after semithin sections positioning. They were then rinsed and post stained with lead citrate and uranyl acetate and imaged under a JEM-1200 EX electron microscope (JEOL Ltd., Tokyo, Japan). Overall, 15–20 randomly selected micrographs per group were obtained at 15000 magnification and analyzed by a blinded investigator. Images of mitochondria

in cell bodies of pulmonary arterial tissue of cells were obtained. Mitochondrial length in cells was measured using Image J software (NIH Image for the Macintosh, Cupertino, California, USA).

2.8 Immunohistochemistry

We used the ultrasensitive systolic pressure and diaminobenzidine staining kits (both from Maixin-Bio, Fuzhou, China) to stain the paraffin-embedded lung tissues and arterial sections. Primary polyclonal antibody was diluted 1:100–200. We incubated the samples with 0.1 M PBS in place of the primary antibody as a negative control. We then used a BX51 microscope (Olympus) to analyze the digital images. In each group, we observed 15 pulmonary arteries from six rats, the external diameter being 60–80 μm. We used average optical density to calculate the protein levels.

2.9 Quantitative real-time reverse transcription-PCR (qRT-PCR) analysis

Total RNA were extracted from pulmonary arterial tissues or cultured cells using Trizol reagent (Invitrogen, Carlsbad, CA, USA) in accordance with the manufacturer's instructions. Quality of isolated RNA was assessed by spectrophotometric analysis (Nanodrop, Wilmington, DE, USA). cDNA was synthesized using the MMLV Reverse Transcriptase kit (Takara Biotechnology, Dalian, China). Real-time PCR was performed with an ABI Prism 7300 system (Applied Bio-systems) using SYBR Premix Ex Taq (Takara Bio, Otsu, Japan).

2.10 Western blot analysis

Protein was extracted from PASMCs and pulmonary arterial tissues with lysis buffer (RIPA buffer: PMSF = 6:1), and equal amounts of protein from each sample (30 μg) were separated by 12% or 10% sodium dodecyl sulfate polyacrylamide gel electrophoresis and transferred to polyvinylidene fluoride membranes. The membranes were then incubated with primary antibodies overnight at 4 °C and horseradish peroxidase-coupled goat anti-rat or anti-rabbit secondary antibody. The chemiluminescence signals were detected with a chemiluminescent HPR substrate (Millipore Corporation, Billerica, USA). The densitometric analysis was conducted with Alpha Imager 2000 (Alpha Innotech Corporation, San Leandro, USA).

2.11 Proliferation assay-Ki-67

The proliferation of PASMCs was determined by Ki-67 staining, and cell number counting. For Ki-67 staining, after fixation, permeabilization, and blocking, PASMCs were incubated with Ki-67 antibody (1:500 dilution, Abcam, Cambridge, MA, USA) and then stained with goat anti-rabbit IgG antibody. For cell number counting, at least 200 cells or 10 images were quantified in each well to get accurate numbers for each group. Finally, cells were detected with a fluorescence microscope.

2.12 Flow cytometric determination of cell cycles

PASMCs were seeded into six-well plates and treated as described above (n = 3 wells/group). Forty-eight hours later, harvested cells were stained with propidium iodide and were subjected to flow cytometric analysis (BD FACS Canto II).

2.13 Immunofluorescence

To determine subcellular distribution of mitochondria, cells were loaded with 50 nM MitoTracker green (Life Technologies, Carlsbad, CA, USA) for 30 minutes to stain the mitochondria. Nuclei were counterstained with 4,6-diamond-2-phenyl insole (DAPI). Images were taken using Olympus FV1000 confocal microscope (Olympus, Tokyo, Japan).

2.14 Terminal deoxynucleotidyl transferase-mediated dUTP nick end labeling (TUNEL) staining

Frozen mice ventricular tissues embedded in optical coherence tomography compound were cut into 4 μm-thick sections and fixed in 4% paraformaldehyde at room temperature. The TUNEL assay was performed followed instructions of the in situ apoptosis detection kit (Roche Diagnostics Ltd., Shanghai, China) and examined using fluorescence microscope. Images were recorded by Olympus BX-51 light microscope at × 400 magnification. Only nuclei that were clearly located in cardiac myocytes were considered. The apoptotic index was presented as the percentage of the number of TUNEL-positively stained nuclei to the number of DAPI-stained nuclei from eight random fields.

2.15 Mitochondrial function study

Pulmonary arterial mitochondria were isolated using the method described previously.[27] Briefly, the minced pulmonary arterial tissue was homogenized in ice cold mitochondrial isolation buffer. The homogenates were used to isolate mitochondria by differential centrifugation. Finally, assessment of mitochondrial reactive oxygen species production, mitochondrial membrane potential change and mitochondrial swelling was performed according to the experimental protocols.

The pulmonary arterial mitochondrial reactive oxygen species production was determined by using fluorescent dye dichlorohydrofluorescein diacetate (DCFDA). The pulmo-

nary arterial mitochondria were incubated at 25 °C with DCFDA for 20 minutes. The reactive oxygen species level was assessed at an excitation/emission wavelength at 485/530 nm using a fluorescent microplate reader (Bio Tek Instruments, Inc., Winooski, Vermont, USA). The increased fluorescent intensity indicates increased mitochondrial reactive oxygen species production.

The pulmonary arterial mitochondrial membrane potential was determined by using the dye 5, 5', 6, 6'-tetrachloro-1, 1', 3, 3'-tetraethylbenzimidazolcarbocyanine iodide (JC-1). The mitochondrial proteins were stained with JC-1 at 37 °C for 30 minutes and then mitochondrial membrane potential was determined as fluorescence intensity by using a fluorescent microplate reader. JC-1 monomer (green fluorescence) and aggregate (red fluorescence) form was excited/emitted at a wavelength of 485/530 nm and 485/590 nm, respectively. A decrease in the red/green fluorescence intensity ratio indicated mitochondrial depolarization.

2.16 Mitochondrial biosynthesis study

The mitochondrial respiratory chain complex V activity was detected by using spectrophotometer. In brief, 100 μL of the sample (containing 10 μg of total mitochondrial protein) was added into the mixture (GENMED buffer, GENMED reagent and GENMED substrate). The total sample activity and sample non-specific activity were immediately detected by spectrophotometer at 340 wavelength from 0 minute to 5 minutes. Calculate sample specific activity: Sample specific activity = Total sample activity - Sample non-specific activity.

The mitochondrial ATPs activity was detected by using spectrophotometer. In brief, 20 μL of the sample (containing 2 μg of total mitochondrial protein) was added into the GENMED buffer (880 μL) at room temperature for 3 minutes and added the GENMED reaction working fluid (100 μL) for three second. The sample reading and background reading were immediately detected by spectrophotometer at 340 wavelength from 0 minute to 1 minute. Calculate the activity of the sample [(sample reading - background reading) × 1 (system capacity: mL) × sample dilution] / [0.02 (sample capacity: mL) × 21.84 (mmoL absorbance) × 1 (reaction time: minute)] = Unit/mg

2.17 Promoter analysis

Rats Drp1 promoter was analyzed for predicted hypoxia response element (HRE) binding sites using MatInspector software (Genomatix Tools). Promoter analysis produced two predicted HRE binding site on Drp1 promoter, which was located 2008 bp and 896 bp upstream the promoter with a score probability of 0.78 and 0.82 (1-highest probability).

2.18 Luciferase assays

After 24 hours, the cells were cotransfected with Drp1 promoter mutation in the absence of HRE, firefly luciferase reporter plasmid, and Renilla luciferase plasmid according to the manufacturer's instructions. Cells were incubated for 24 hours under hypoxia condition, and using normoxia condition as a control group. Then, cell lysates were prepared and luciferase activities were measured using the dual-luciferase reporter assay system (Promega, Madison, WI). Firefly luciferase activity was normalized to the activity of Renilla luciferase.

2.19 Chromatin immunoprecipitation (ChIP)

ChIP assay was performed using chromatin from fixed PASMCs in 1% formaldehyde and was sonicated in a Bioruptor System (Diagenode, USA) which let us to obtain DNA fragments between 200 bp and 1000 bp in size. After sonication, the protein-DNA complexes were immunoprecipitated using anti-ICAM (as negative control), anti-RNA poll 2 (as positive control) and anti-HIF-1α antibodies. After cross-linking reversal at 65 °C for 4 hours, DNA was purified using the phenol-chloroform method. Primers (5' to 3') for end-point PCR or quantitative real-time PCR were as follows: HIF-1α-Fw-GTGCTGGACCGCTTTTACAATGC, Rv-CAGTTCAAGTCG ATCGCATGGAC. Input (diluted 1/300) was used as a normalizing control.

2.20 Statistical analyses

Statistical analysis was performed using SPSS18.0 software. The data were presented as mean ± SD. For comparison of two groups, *t*-tests (two-tailed) were performed; for multiple groups (three or more groups), one-way analysis of variance and post hoc statistical comparisons with the Bonferroni adjustment were conducted. A *P*-value of < 0.05 was considered statistically significant.

3 Results

3.1 HIF-1α regulates the pathogenesis of hypoxic PH

Previous studies have shown that hypoxia is the critical common mediator in the development of PH. Hypoxia also can promote the transcription factor HIF-1α. Therefore, we examined whether HIF-1α was activated in hypoxia-induced pulmonary vascular remodeling and PH development. Hemodynamic and vascular remodeling parameters were measured in male rats exposed to hypoxia or normoxia for four weeks. Hypoxia significantly increased mPAP, RVSP, medial wall thickness, and RV/(LV + S) in rats following four weeks of exposure (Figure 1A–F). In hypoxia-induced rats, we observed that HIF-1α expression in the lung tissue

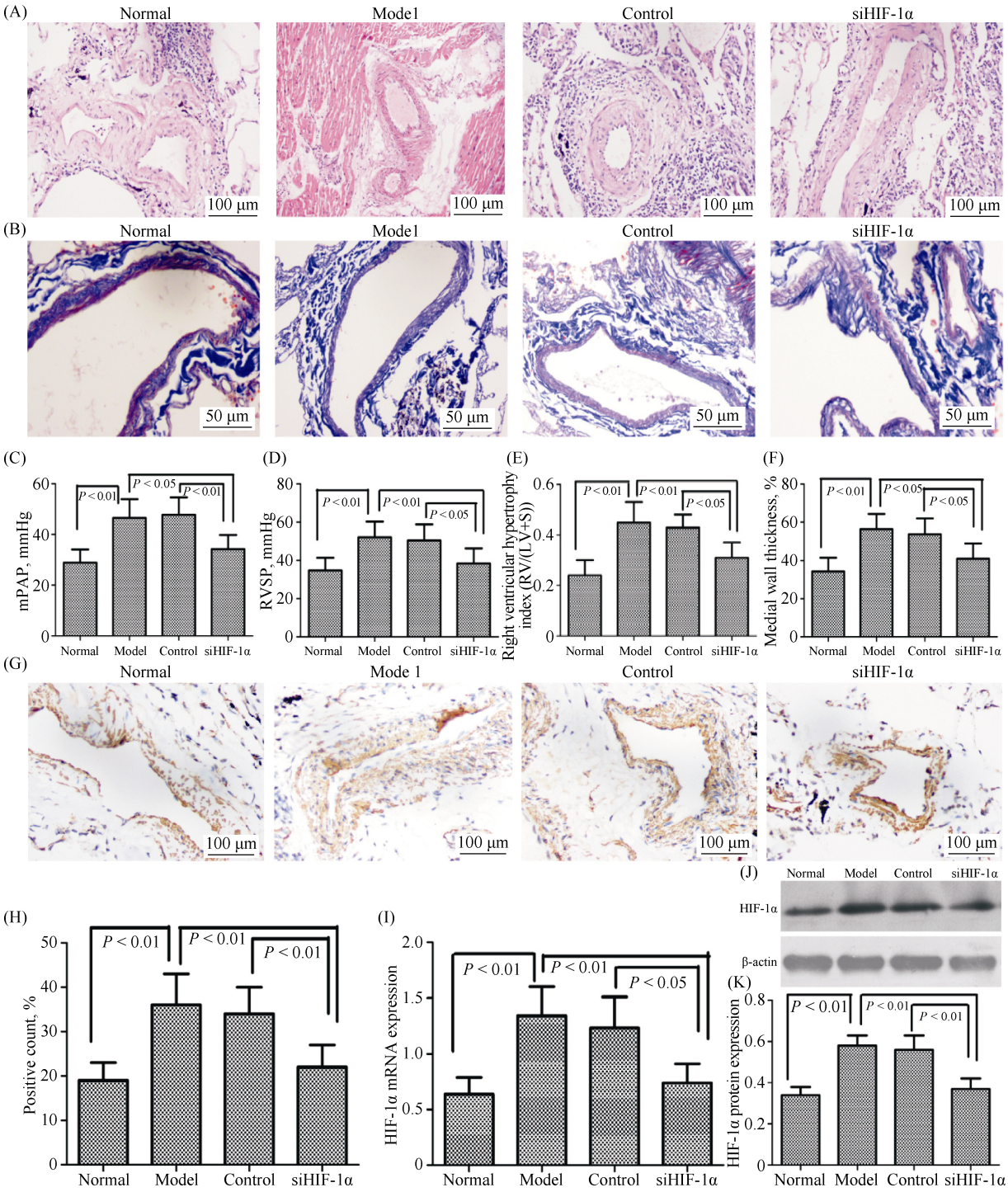

Figure 1. HIF-1α regulates the pathogenesis of hypoxic pulmonary hypertension. (A): Representative images of hematoxylin-eosin staining (H & E) in lung tissues lesions, magnification 400 × (n = 6). Ten pulmonary arterioles were randomly examined for the structural integrity from hematoxylin-eosin staining images of lung tissues lesions by Image J software; (B): representative images of Masson staining in lung tissues lesions, magnification 400 ×; (C–D): right heart catheterization analysis of mPAP and RVSP on the surviving rats; (E): the degree of right ventricular hypertrophy expressed as RV/(LV + S); (F): the measurement of medial wall thickness of distal pulmonary vessels; (G–H): lung tissue sections were stained for HIF-1α (magnification, 200 ×); and (J–L): immunoblots of HIF-1α using pulmonary arteries isolated from the rats exposed to either normoxia or hypoxia. siHIF-1α, lentiviral vector-mediated short-hairpin RNA targeting HIF-1α; Control, lentiviral vector containing scramble siRNA. HIF-1α: hypoxia-inducible factor-1α; LV: left ventricle; mPAP: mean pulmonary arterial pressure; RV: right ventricle; RVSP: right ventricular systolic pressure; S: septum; siHIF-1α: small interfering hypoxia-inducible factor-1α; siRNA: small interfering RNA.

was increased during the PH development phase (Figure 1G–J). The silencing of HIF-1α attenuated hypoxia-induced vascular remodeling which significantly decreased mPAP, medial wall thickness, RVSP and RV/(LV + S) in the rats (Figure 1A–F). However, this hypoxia-induced HIF-1α expression was abolished in small interfering HIF-1α (si-HIF-1α) rats (Figure 1G–J). These results demonstrated that the suppression of HIF-1α expression by siRNA attenuated the symptoms of hypoxia- induced PH and pulmonary vascular remodeling.

3.2 HIF-1α is involved in hypoxia-induced proliferation and apoptosis of PASMCs

PASMC proliferation and apoptosis are essential steps of vascular remodeling in PH. Therefore, we addressed whether transfection with HIF-1α siRNA affected PASMC proliferation and apoptosis as assessed by Ki-67 staining, cell number counting, and flow cytometry assays. As shown in Figure 2, PASMC proliferation was significantly enhanced in cells exposed to hypoxia; however, the apoptosis index of PASMCs under hypoxic conditions was significantly decreased. Application of siHIF-1α significantly blocked the hypoxia-induced enhancement of PASMCs proliferation and abrogated PASMCs apoptosis, and this hypoxia-induced HIF-1α expression was abolished in siHIF-1α rats (Figure 2A–D). These data suggested that the proliferation and apoptosis of PASMCs were directly regulated by HIF-1α in response to hypoxia.

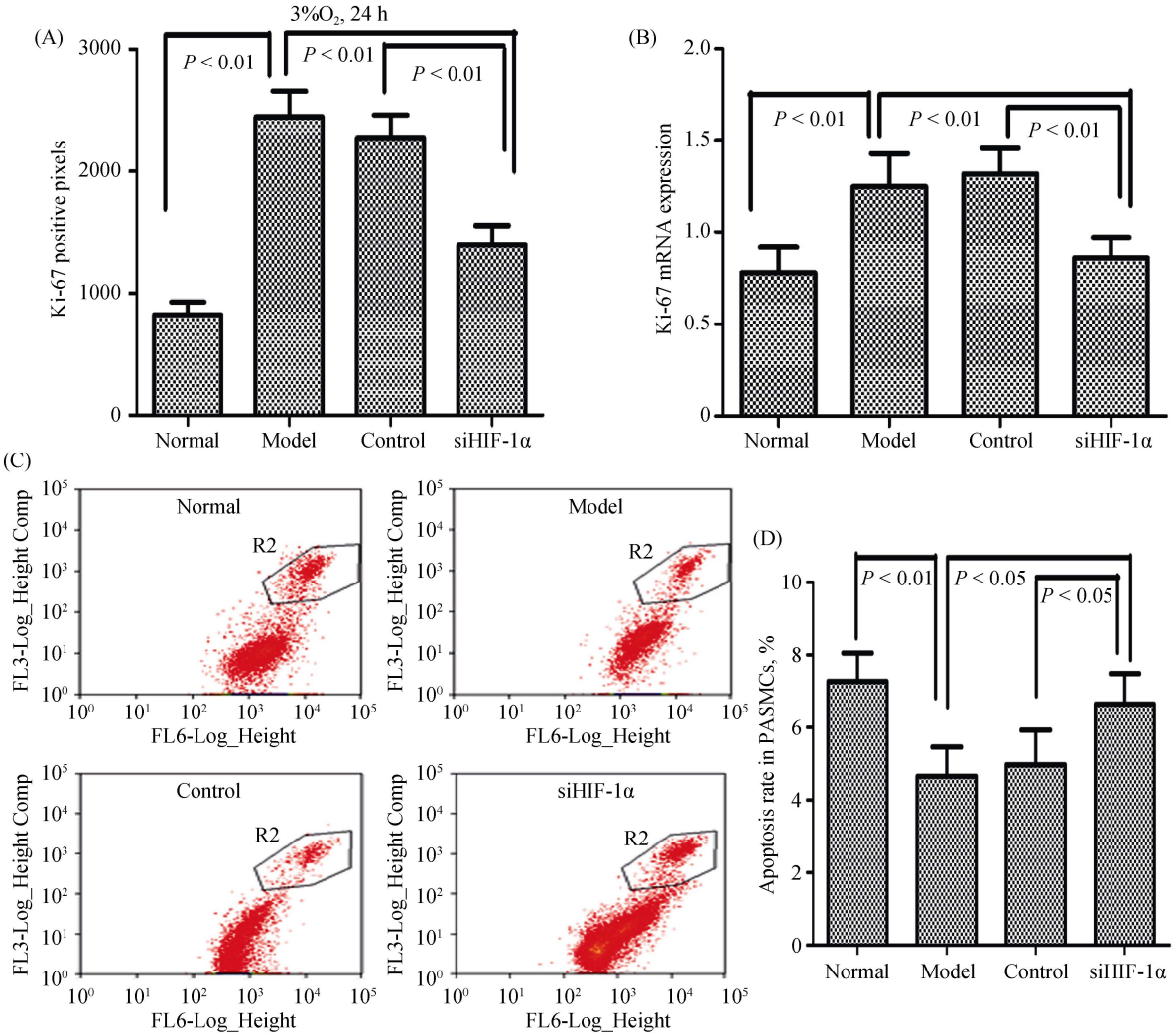

Figure 2. HIF-1α is involved in hypoxia-induced proliferation and apoptosis of PASMCs. PASMCs were infected with lentiviruses harboring HIF-1α siRNA or scramble siRNA, and exposed to hypoxia (3% O_2) for 24 hours. (A & B): The number of proliferation cells was determined by Ki-67 assay in cell number counting and expression of Ki-67 mRNA in the qRT-PCR; and (C–D): the cells were fixed and stained with propidium iodide, and cell cycle was analyzed by flow cytometry. A set of representative flow cytometry results (C), and statistical analysis of three independent experiments (D). HIF-1α: hypoxia-inducible factor-1α; PASMCs: pulmonary arterial smooth muscle cells; qRT-PCR: quantitative real-time polymerase chain reaction; siHIF-1α: small interfering hypoxia-inducible factor-1α; siRNA: small interfering RNA.

3.3 Morphology and function of mitochondria under hypoxia is dependent on HIF-1α

Mitochondrial morphologic changes were detected by electron microscopy. Smaller and fatter mitochondria were seen in the PH group, while these pathological changes were significantly attenuated in the siHIF-1α group (Figure 3A). The number of mitochondrial and the acreage of mitochondrial were significantly increased, while the ratio of mitochondrial length/width was significantly reduced in PH lung vascular tissue compared to the normoxic group. Conversely, siHIF-1α significantly increased the ratio of mitochondrial length/width, and reduced the number of mitochondrial and the acreage of mitochondrial (Figure 3B). We further observed the mitochondrial morphologic changes in PASMCs. Most of the mitochondria were fragments or scattered points under hypoxic conditions, while siHIF-1α could significantly recover the pip network structure (Figure 3C).

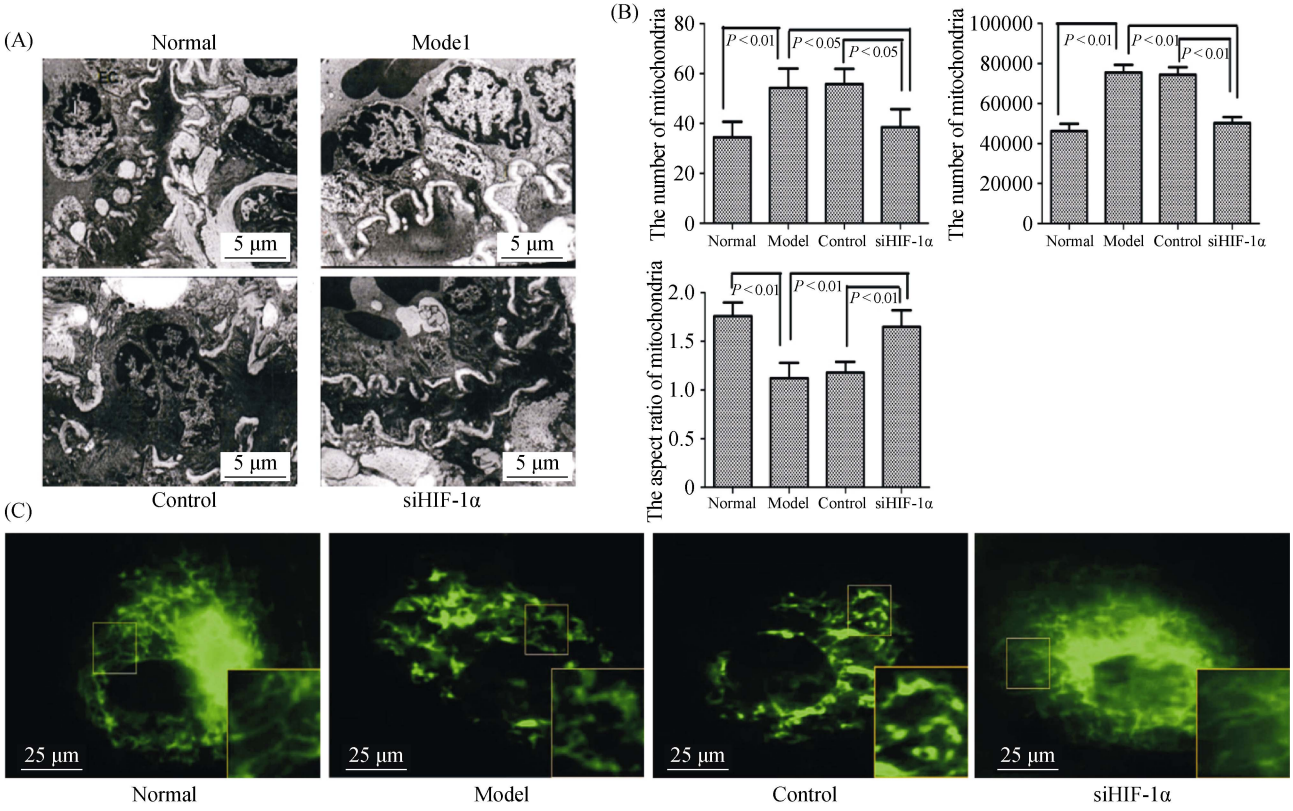

Figure 3. The morphology of mitochondria under hypoxia is dependent on HIF-1α *in vivo* and *in vitro*. (A): Representative electron micrograph of lung tissues lesions in different groups (magnification, 10000 ×); (B): graphs indicate the mitochondria number, per area and average mitochondrial size; and (C): electron micrographs of mitochondria in PASMCs (magnification, 1000 ×). The normal group displayed elongated mitochondria, whereas the hypoxia model group displayed short or spherical shaped mitochondria. The administration of siHIF-1α markedly attenuated mitochondrial fragmentation in the PASMCs of hypoxia. HIF-1α: hypoxia-inducible factor-1α; PASMCs: pulmonary arterial smooth muscle cells; siHIF-1α: small interfering hypoxia-inducible factor-1α.

Since mitochondrial shape changes might lead to impaired respiratory enzyme activity and energy production in tissues, we next evaluated mitochondrial function by measured key enzyme activity associated with respiratory chain and ATP levels. We found that the ratio of mitochondrial DNA/nuclear DNA, Complex IV activity, and ATPs activity levels were significantly reduced in mitochondria of PH rats compared with normal rats; observations that were significantly increased by siHIF-1α treatment (Figure 4A–C). Our results thus demonstrated that mitochondrial shape changes were correlated with decreases of mitochondrial respiratory enzyme activity and ATP abundance in hypoxic pulmonary arterial hypertension.

In PH, PASMCs have dysmorphic mitochondria with reduced respiratory chain coupling, inefficient use of oxygen, and increased glycolysis. To determine whether PASMCs have similar alterations, we used MitoTracker to capture mitochondrial morphologic features and measure production of mitochondrial-derived ROS and JC-1 staining method to detect mitochondrial membrane potential. Compared with

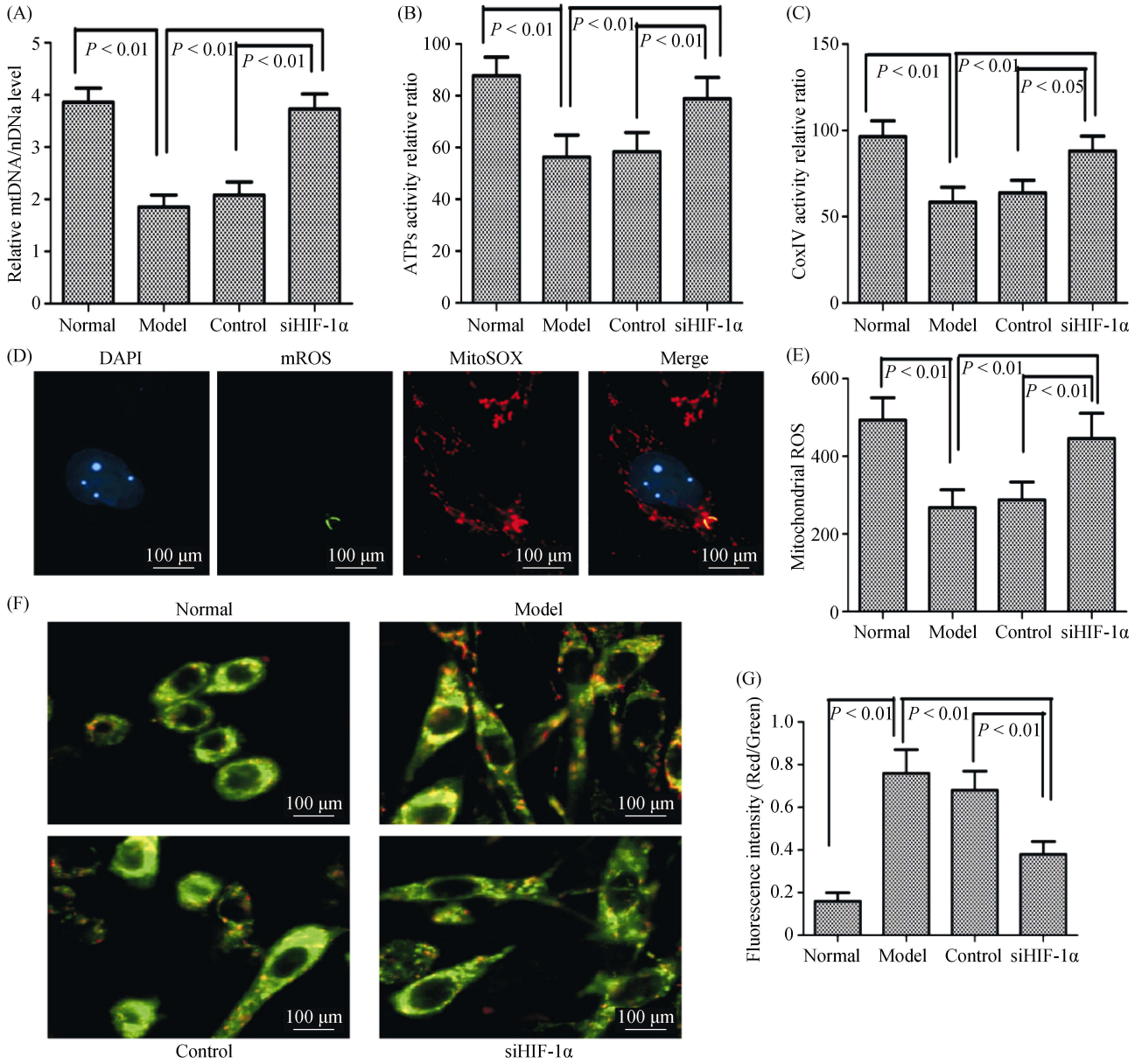

Figure 4. The mitochondrial biogenesis and function under hypoxia is dependent on HIF-1α *in vivo* and *in vitro*. (A): The relative mitochondrial DNA copy number was determined by comparison to nuclear DNA (rRNA 18S); (B): ATPs activity relative was measured by using spectrophotometer in different conditions; (C): complex IV activity relative was measured by using spectrophotometer in different conditions; (D): the ROS was detected by using fluorescent dye dichlorohydrofluorescein diacetate assay (magnification, 400 ×); (E): measurement of ROS generation in different conditions; (F): MMP as determined using the JC-1 assay (magnification, 400 ×); and (G): MMP as determined using the JC-1 assay kit in different conditions. ATPs: adenosine triphosphates; DAPI: 4,6-diamond-2-phenyl insole; HIF-1α: hypoxia-inducible factor-1α; MMP: mitochondrial membrane potential; ROS: reactive oxygen species; siHIF-1α: small interfering hypoxia-inducible factor-1α.

the normoxic group, PASMCs under hypoxia significantly reduced ROS production in the cytoplasm (Figure 4D–E), and significantly increased mitochondrial membrane potential, as indicated by the red/green fluorescent intensity ratio (Figure 4F–G). In addition, ROS production significantly increased, while the mitochondrial membrane potential was significantly reduced by knockdown of HIF-1α. These results indicated that mitochondrial dynamics were involved in hypoxia-induced pulmonary vascular remodeling by HIF-1α regulation.

3.4 Expression of mitochondrial dynamics proteins is regulated in pulmonary vascular remodeling by HIF-1α

Mitochondrial morphology is regulated by a family of

mitochondrial fusion and fission proteins. We therefore investigated expression of fusion proteins (Mfn1, Mfn2 and OPA1) and fission proteins (Drp1 and Fis1) in PH rats and PASMCs by Western blotting and qRT-PCR analysis (Figure 5A–F). There were no detectable changes in the expression of fission protein Fis1 levels between the normoxia and hypoxia groups both *in vivo* and *in vitro*. However, there was significantly increase in fission protein Drp1 expression

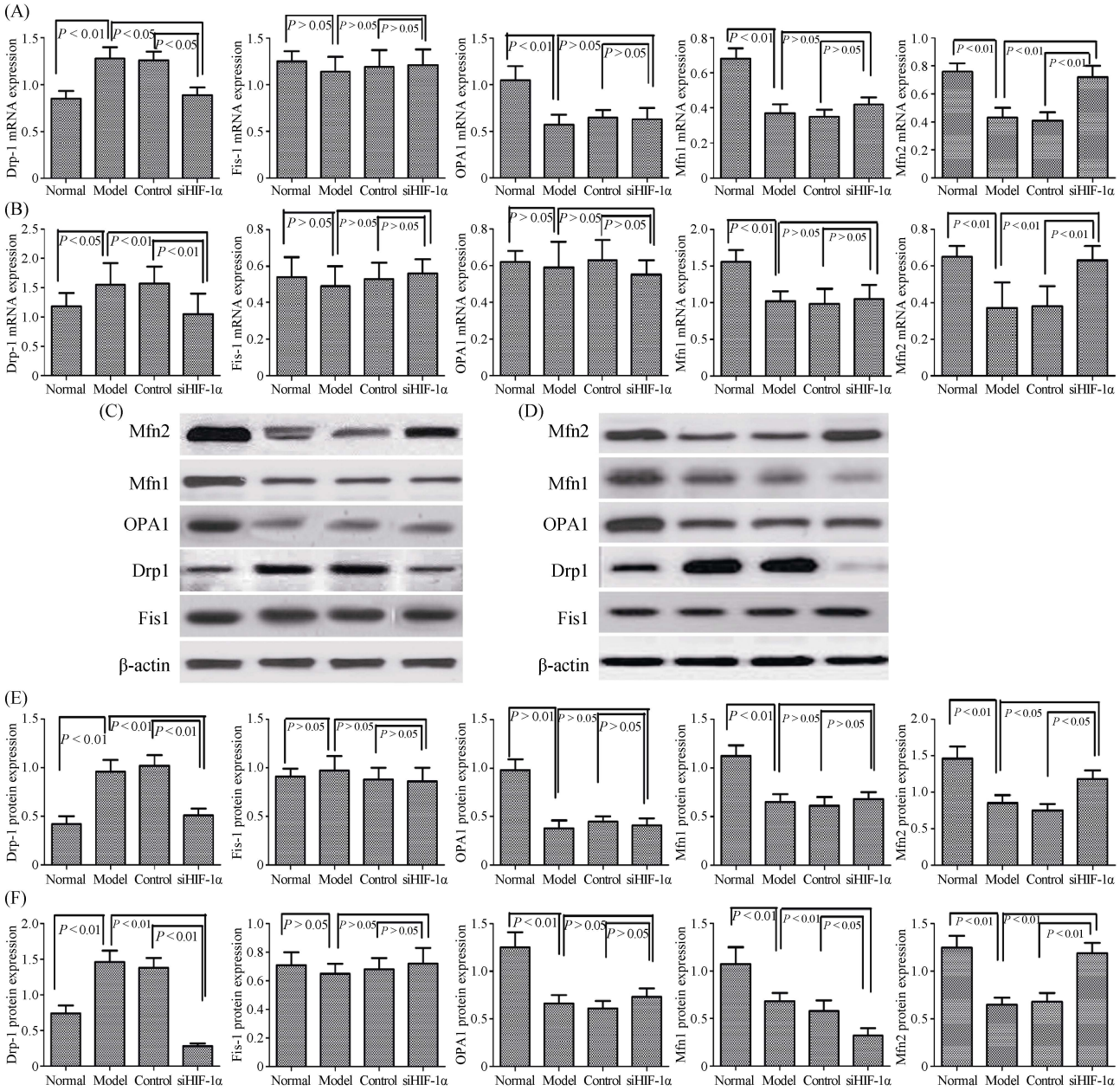

Figure 5. Expression of mitochondrial dynamics proteins is regulated in pulmonary vascular remodeling by HIF-1α. (A): The expression of mitochondrial fission and fusion mRNA in lung tissue were measured by the qRT-PCR; (B): the expression of mitochondrial fission and fusion mRNA in PASMCs were measured by the qRT-PCR; (C): the expression of mitochondrial fission and fusion protein in lung tissue were measured by the Western Blot analysis; (D): the expression of mitochondrial fission and fusion protein in PASMCs were measured by the Western Blot analysis; (E): the changes of mitochondrial fission and fusion protein in lung tissue were significantly different from the normoxia group; and (F): the changes of mitochondrial fission and fusion protein in PASMCs were significantly different from the normoxia group. Drp1: dynamin-related protein 1; Fis1: fission 1; HIF-1α: hypoxia-inducible factor-1α; Mfn1: mitofusin 1; Mfn2: mitofusin 2; OPA1: optic atrophy 1; PASMCs: pulmonary arterial smooth muscle cells; qRT-PCR: quantitative real-time polymerase chain reaction; siHIF-1α: small interfering hypoxia-inducible factor-1α.

levels between normoxia and hypoxia *in vivo* and *in vitro*. This suggested that mitochondrial fission protein Drp1 was involved in pulmonary vascular remodeling. We also found that the expression of fusion proteins Mfn2, Mfn1, and OPA1 were significantly reduced compared with normoxia groups in PH rat pulmonary arterial tissue and PASMCs. We analyzed mRNA expression of Mfn1, Mfn2, and OPA1, and found no detectable changes in fusion protein OPA1 mRNA levels between normoxia and hypoxia in PASMCs. However, we found that levels of Mfn1 and Mfn2 mRNA decreased significantly upon hypoxia exposure compared with the normoxia exposure in PASMCs. These results suggested that mitochondrial fusion protein Mfn1and Mfn2 were involved in pulmonary vascular remodeling.

To demonstrate the effects of downregulation of HIF-1α in hypoxic conditions, siRNA was used to study the effects of HIF-1α knockdown on PH rats and PASMCs. The mRNA and protein expression levels of fission protein Drp1 was significantly downregulated in the HIF-1α group, as compared with the scramble and hypoxia groups (Figure 5A–F). In addition, no difference was observed between the scrambled and hypoxia groups. As presented in Figure 5, the mRNA and protein expression levels of Mfn2 was also upregulated in the HIF-1α group, as compared with the scramble and hypoxia groups. These results indicated that knockdown of HIF-1α resulted in a marked decrease Drp1 and increase Mfn2 in the mRNA and protein expression levels.

3.5 HIF-1α regulates mitochondrial function via Drp1 in PASMCs

Our data thus far had suggested that postnatal HIF-dependent mitochondrial dynamics could be mediated by increases in Drp1 and decrease in Mfn2 expression. We therefore analyzed the expression of Drp1 in the pulmonary vascular tissue of rats with hypoxic PH via immunohistochemistry, and the results were consistent with the protein analysis from Western blotting (Figure 6A–B). We further confirmed that the co-localization expression of HIF-1α and Drp1 in lung tissue and PASMCs by immunofluorescence (Figure 6C–D). The results suggested that a direct interaction between HIF-1α and Drp1 might exist, but the specific mechanism requires further investigation.

We further examined whether HIF-1α bound to the 5' promoters of Drp1. To achieve this, we analyzed published 5' promoter sequences for the Drp1 gene, and found several canonical (A/G) CGTG HIF-1α binding sites in each case (Figure 6E). We assayed whether HIF1α directly bound these promoters using anti-HIF-1α serum to perform chromatin immunoprecipitation and luciferase reporter gene assay. We found that in each case, chromatin containing at least one HIF-1α-binding site promoter fragment was enriched over non-amplified sequences in chromatin from PASMCs (Figure 6F–I), implying that HIF-1α bound to these sites *in vivo*. These results suggested that HIF-1α directly interacted with target gene Drp1 under hypoxic conditions and might be involved in transcriptional regulation by modulating the Drp1 promoter hypoxic reaction element.

3.6 Mitochondrial dynamics is involved in the hypoxia-induced promotion of pulmonary vascular remodeling via Drp1

The role of Drp1 on mitochondrial dynamics was further explored in hypoxia-induced promotion of pulmonary vascular remodeling. We used the Drp1 specific inhibitor, Mdivi-1, to inhibit the Drp1 expression *in vivo* and *in vitro*. We treated hypoxia-induced PH rats with Mdivi-1 by intraperitoneal injection. Hemodynamic and vascular remodeling parameters analysis showed that Mdivi-1 treatment reduced the mPAP, RVSP, medial wall thickness and RV/(LV + S), as demonstrated by hematoxylin-eosin and Masson staining (Figure 7A–D). Analyses of PCNA and Caspase-3 expression, and TUNEL assay were conducted on paraffin-embedded rat lung tissues. The results showed a decreased number of PCNA-positive cells in the pulmonary artery media, whereas TUNEL-positive cells and Caspase-3 were dramatically increased following Mdivi-1 injection (Figure 7E–I). Taken together, the results indicated that mitochondrial dynamics exerted pro-proliferative and anti-apoptotic effects on vascular smooth muscle under hypoxia via Drp1.

We next investigated whether the mitochondrial dynamics were involved in the proliferation and apoptosis of PASMCs via Ki-67 and flow cytometry assays. As shown in Figure 8A–D, PASMC proliferation was significantly reduced in cells treated with Drp1 specific inhibitor, Mdivi-1; however, the apoptosis index of PASMCs treated with Mdivi-1 was obviously enhanced. The results suggested that expression of PCNA was decreased in PASMCs, whereas the expression of Caspase-3 was dramatically increased following Mdivi-1 (Figure 8E–J). Taken together, the results indicated that mitochondrial dynamics exerted pathogenic-promoting effects during hypoxia-induced pulmonary vascular remodeling via Drp1.

4 Discussion

The major finding of our study was that HIF-1α upregulation correlated with advanced hypoxia-induced pulmonary vascular remodeling in rats. We demonstrated that HIF-1α

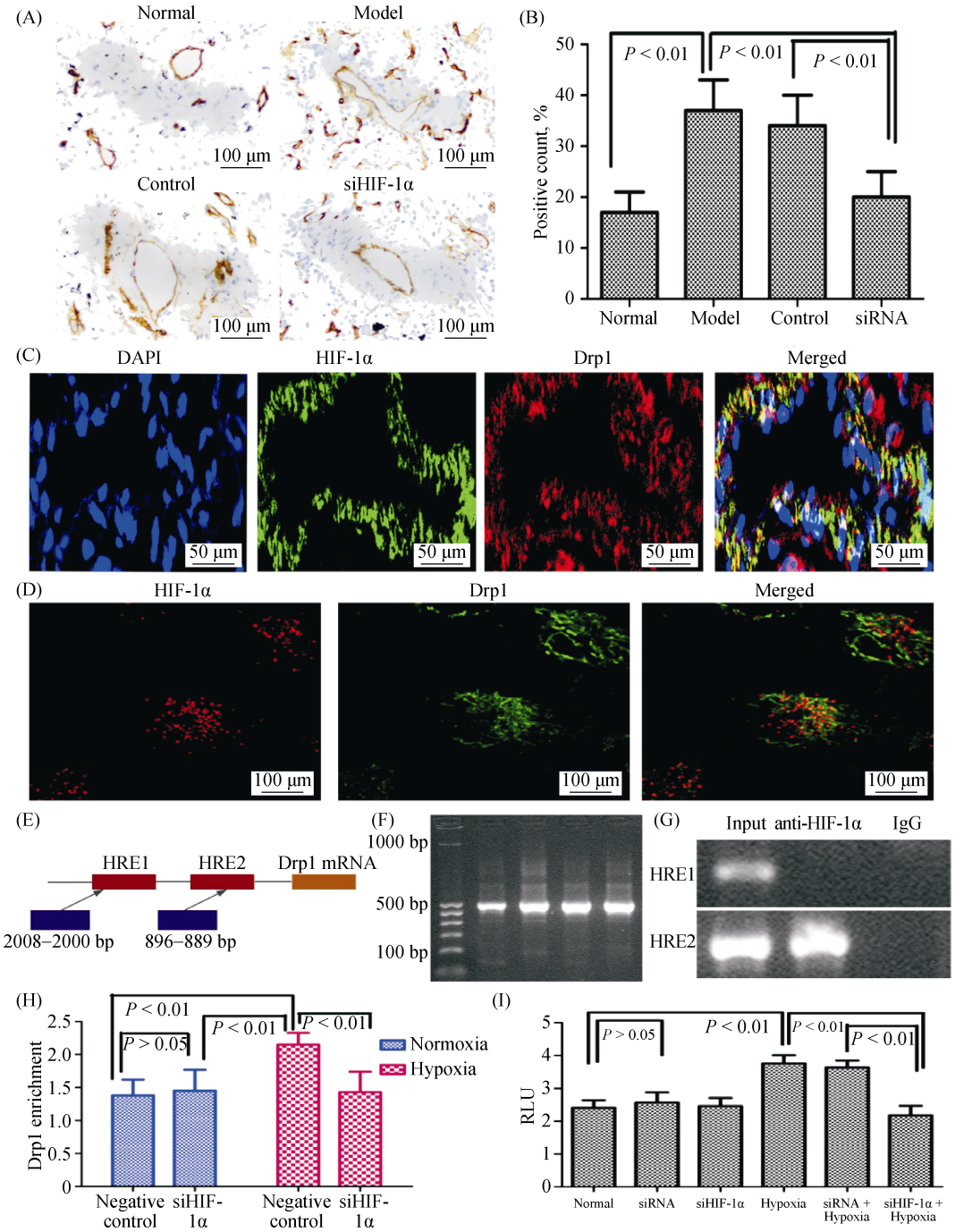

Figure 6. HIF-1α regulates mitochondrial function by Drp1 under hypoxia. (A–B): Immunohistochemical evaluation of the expression of Drp1 in lung. Drp1 expression was increased in pulmonary vessels with hypoxia (magnification, 200 ×); (C): the sections were stained with Drp1 antibody (red) and co-stained with HIF-1α antibodies to demonstrate adventitia (green), DAPI to demonstrate cell nuclear (blue), respectively. Immuno-reactive Drp1 and HIF-1α were expressed both in the pulmonary vascular media and in the intima, and more intensively in the smooth muscle layer (magnification, 400 ×); (D): the PASMCs were stained with Drp1 antibody (red) and co-stained with HIF-1α antibodies to demonstrate adventitia (green), respectively. Immunoreactive Drp1 and HIF-1α were expressed both in PASMCs of mitochondrial under hypoxic conditions (magnification, 400 ×); (E): schematic diagram showing the hypoxic reactive elements in the promoter region of Drp1; (F–G): the levels of Drp1 promoter with HIF-1α in PASMCs were detected by chromatin immunoprecipitation assay; (H): the transcriptional activity of Drp1 promoter under hypoxia was detected by luciferase reporter gene; and (I): the effect of endogenous HIF-1 alpha expression on the activity of Drp1 promoter in siRNA PASMCs. DAPI: 4,6-diamond-2-phenyl insole; Drp1: dynamin-related protein 1; HIF-1α: hypoxia-inducible factor-1α; PASMCs: pulmonary arterial smooth muscle cells; siHIF-1α: small interfering hypoxia-inducible factor-1α; siRNA: small interfering RNA.

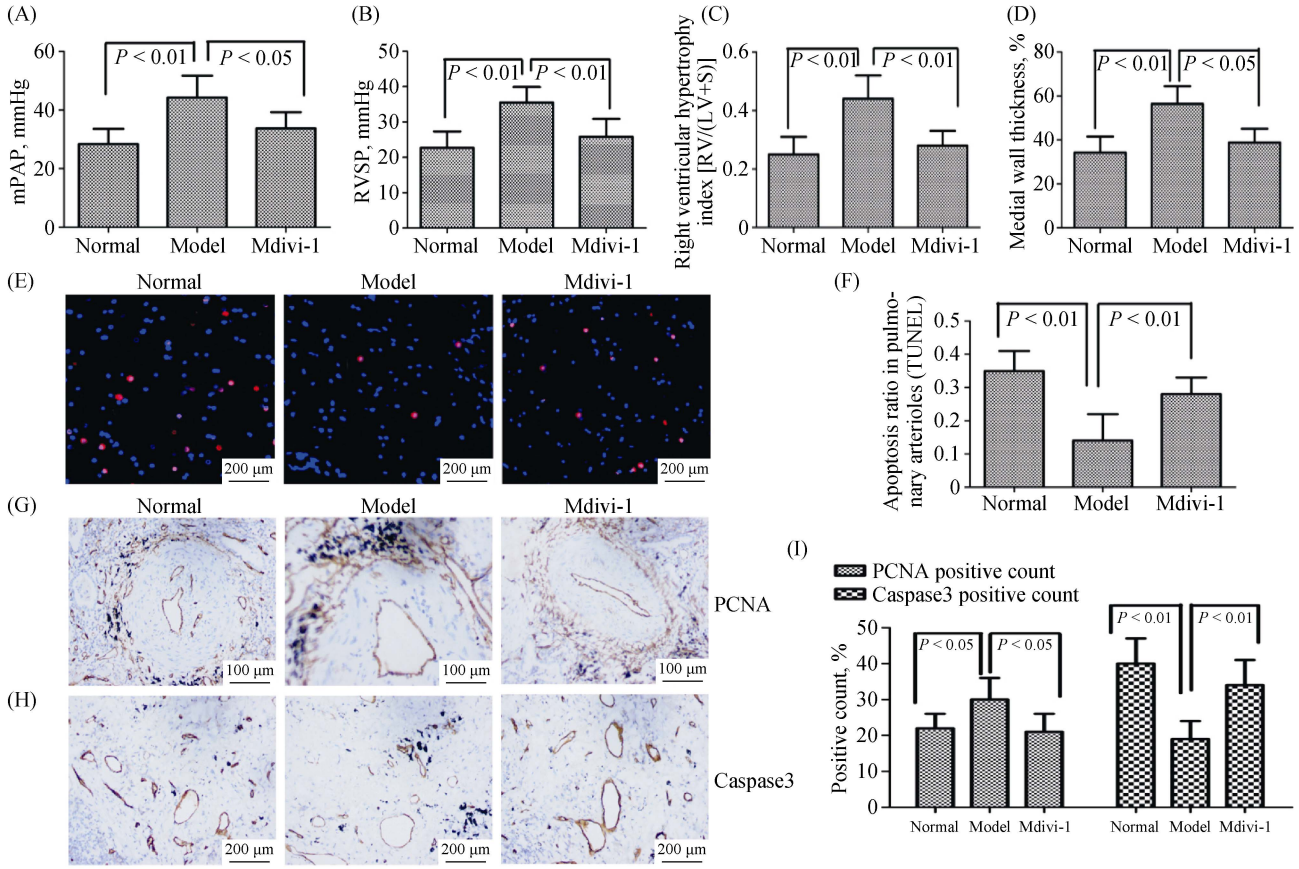

Figure 7. The mitochondrial dynamics is involved in the hypoxia-induced promotion of pulmonary vascular remodeling via Drp1. (A–B): Right heart catheterization analysis of mPAP and RVSP on the surviving rats; (C): the degree of right ventricular hypertrophy expressed as RV/(LV + S); (D): the measurement of medial wall thickness of distal pulmonary vessels; (E–F): representative images of TUNEL staining for the different experimental groups. Nuclei with red staining indicate TUNEL-positive cells (magnification, 400 ×); (G): immunohistochemical evaluation of the expression of PCNA in lung tissue (magnification, 200 ×); (H): immunohistochemical evaluation of the expression of Caspase 3 in lung tissue (magnification, 200 ×); and (I): Caspase 3 expression was decreased in pulmonary vessels with hypoxia, and PCNA expression was increased in pulmonary vessels with hypoxia. Drp1: dynamin-related protein 1; LV: left ventricle; mPAP: mean pulmonary arterial pressure; PCNA: proliferating cell nuclear antigen; RV: right ventricle; RVSP: right ventricular systolic pressure; S: septum.

facilitated PASMCs proliferation and inhibited apoptosis under hypoxia. We also showed that mitochondrial dynamics were involved in the pulmonary vascular remodeling under hypoxia *in vivo* and *in vitro*. Furthermore, HIF-1α also modulated mitochondrial dynamics in pulmonary vascular remodeling under hypoxia by directly regulating the expression of Drp1.

HIF-1α has been demonstrated to play an essential role in the pathophysiology of chronic hypoxia-induced PH in mice with the heterozygous deletion of HIF-1α,[28] and in mice with the smooth muscle-specific disruption of HIF-1α.[29] Recently, HIF-1α was implicated in several molecular mechanisms accounting for the pathogenesis of PH.[30–33] In addition, the increased expression of HIF-1α has been found in the pulmonary arteries of many patients with idiopathic PH.[34,35] Although HIF-1α is recognized as a key player in PH, surprisingly, the potential of HIF-1α as a therapeutic target in the treatment of PH has seldom been illuminated in previous studies.[36] In our study, we applied a lentivirus-mediated gene delivery approach to introduce HIF-1α shRNA to the pulmonary vessels in rats, and showed that the inhibition of the expression of HIF-1α in the pulmonary arteries effectively alleviated chronic hypoxia-induced PH and pulmonary vascular remodeling. In addition, the suppression of HIF-1α expression in primary PASMCs by siRNA significantly reduced the hypoxia-induced acceleration of the proliferation and depressed apoptosis of PASMCs, illustrating that the HIF-1α-regulated proliferation and apoptosis of PASMCs under hypoxic conditions may play an important role in the development of hypoxic PH.

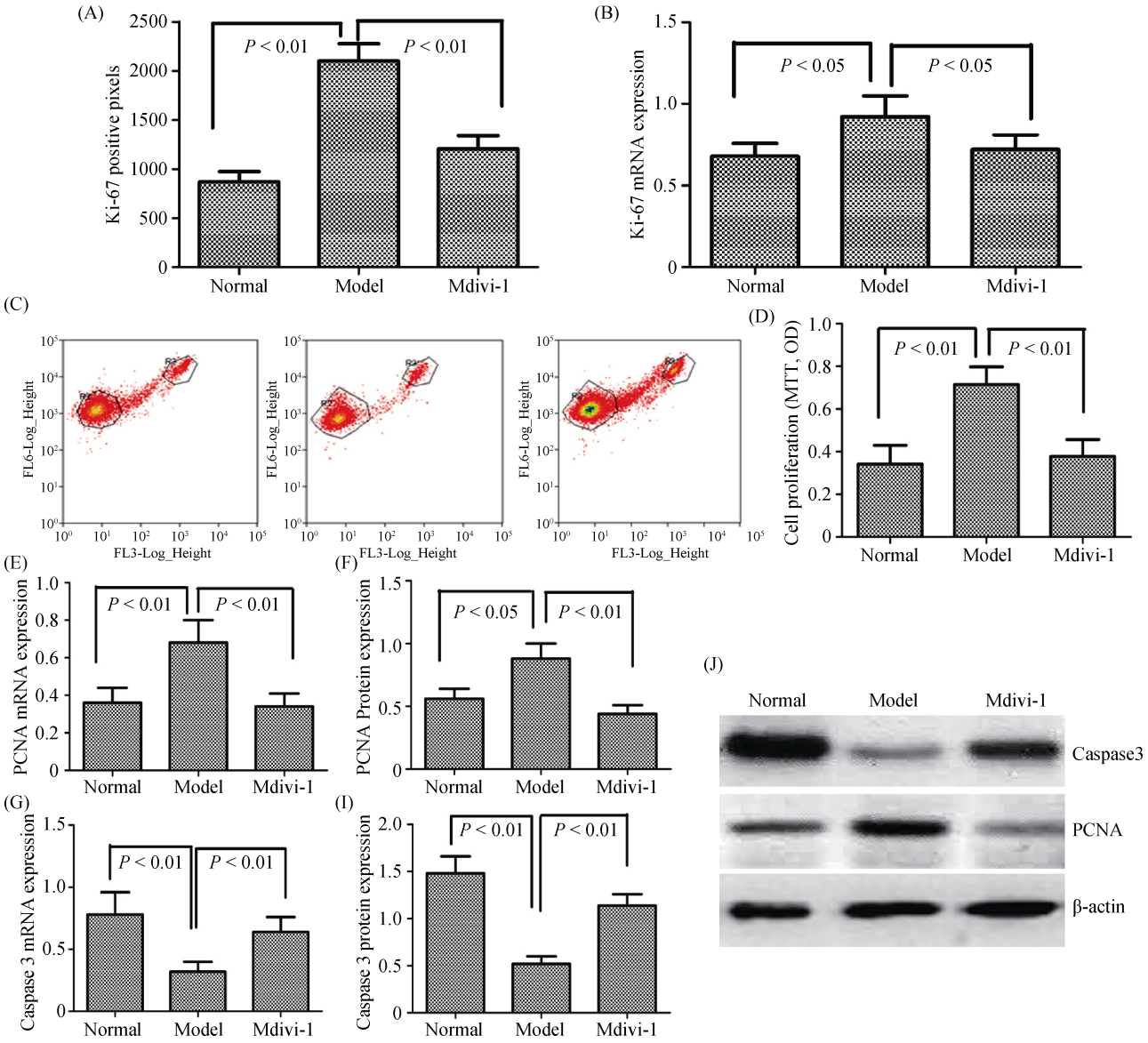

Figure 8. Mitochondrial dynamics are involved in hypoxia-induced proliferation and apoptosis of PASMCs via Drp1. (A): The number of proliferation cells was determined by Ki-67 assay; (B): the expression of Ki-67 mRNA in PASMCs were measured by the qRT-PCR; (C–D): the cells were fixed and stained with propidium iodide, and cell cycle was analyzed by flow cytometry. A set of representative flow cytometry results (C), and statistical analysis of three independent experiments (D); (E): the expression of PCNA mRNA in PASMCs was measured by qRT-PCR; (F): the expression of Caspase 3 mRNA in PASMCs was measured by qRT-PCR; (G): the expression of PCNA protein in PASMCs was measured by Western Blot; (I): the expression of Caspase 3 protein in PASMCs was measured by Western Blot; and (J): the relative expression of protein was determined by comparison to β-actin as the loading control. Drp1: dynamin-related protein 1; PASMCs: pulmonary arterial smooth muscle cells; PCNA: proliferating cell nuclear antigen; qRT-PCR: quantitative real-time polymerase chain reaction.

Mitochondrial dysfunction has long been linked to the pathogenesis of neurodegenerative diseases, diabetes, myopathies, and other human diseases.[37,38] The dysfunction is largely dependent on mitochondrial fission and fusion relative proteins expression, which is critical for mitochondrial homeostasis and cell survival.[39] The balance between mitochondrial energy production and physiological functions required for cell survival is regulated by mitochondrial dynamics.[40] The processes of mitochondrial biogenesis, fission, fusion, and mitophagy regulate the maintenance of mitochondrial mass and the numbers of mitochondria in cells.

Here, we found that mitochondrial fragmentations or smaller mitochondria increased in hypoxia, as observed via

transmission electron microscopy, which indicated that mitochondrial fission was upregulated and this alteration was improved by hypoxia. To better define the change of mitochondria function, we examined mitochondrial DNA (mtDNA) content, complex IV activity, ATPs activity levels, ROS, and mitochondrial membrane potential *in vivo* and *in vitro*. Measurement of lung tissue and PASMCs mitochondrial functional capacity indicated significantly reduced activity of mitochondrial respiration complex IV and ATP, lowered ROS content, and downregulated mtDNA content post hypoxia stimulation, indicating hypoxia-induced impairments in energy metabolism and respiratory complex enzyme activity. Those results can lead to a downstream cascade of mitochondrial depolarization, aberrant calcium handling, impaired ATP synthesis, and activation of proliferation and apoptosis in PASMCs, finally resulting in pulmonary vascular remodeling.

HIF family members play important roles in response to hypoxia, among which HIF-1α is the key factor modulating various downstream genes transcription during the progression of hypoxia pulmonary hypertension (HPH).[41] Here, we found that HIF-1α was involved in the regulation of mitochondrial morphology and function. This conclusion was supported by the findings that HIF-1α inhibition induced mitochondrial swelling and led to mitochondrial dysfunction and apoptosis. Mitochondrial dynamics and morphology are finely tuned by the mitochondrial fusion and fission proteins Mfn1, Mfn2, Fis1, Drp1, and OPA1.[42,43] We found that HIF-1α inhibition affected the expression levels of all of these proteins. In particular, HIF-1α inhibition significantly decreased the expression of Drp1 and increased the expression of Mfn2, which led to changes in mitochondrial morphology and mitochondrial dysfunction. Taken together, these results indicate that hypoxia facilitates mitochondria dysfunction and disruption in pulmonary vascular remodeling through HIF-1α regulated the expression of Drp1 and Mfn2.

The underlying mechanisms may be related to Drp1-mediated mitochondrial fission that is involved in pulmonary vascular remodeling. Previous studies showed that targeting mitochondrial fission Drp1 by mitochondrial division inhibitor Mdivi-1 was effective in PH model rats.[18,44] It is also known that hypoxia-induced mitochondrial fragmentation contributes to the alterations of both PASMC death and proliferation, which could be significantly reduced by Mdivi-1.[45] The above findings thus help explain the Drp1-related working mechanism of hypoxia, in that HIF-1α inhibition might be effective for treating pulmonary vascular remodeling from hypoxia etiologies.

Drp1 is a GTPase that binds to the mitochondrial outer membrane and regulates mitochondrial division.[46] Genetic silencing of Drp1 and the expression of a dominant-negative version of Drp1 each significantly increases mitochondrial length in both neurons and non-neuronal cells.[47] However, it is unlikely that the loss of Drp1 function always leads to increased mitochondrial length. Here, we found that the inhibition of HIF-1α inhibition induced mitochondrial swelling instead of mitochondrial elongation. The mitochondrial swelling in HIF-1α inhibition cells was likely induced by the inhibition of Drp1, since the expression of Drp1 was inhibited in HIF-1α inhibition cells, and the overexpression of Drp1 decreased the mitochondrial swelling in HIF-1α inhibition cells. Consistent with our results, the inhibition expression of Drp1 by mitochondrial division inhibitor Mdivi-1 has been shown to induce mitochondrial swelling, providing further evidence that the loss of Drp1 function can cause mitochondrial swelling, leading to pulmonary vascular remodeling.

In our study, we report that HIF-1α can upregulate Drp1 expression. Our results suggested that HIF-1α was involved in the regulation of Drp1 expression in response to hypoxia. We further verified one functional HRE in the positive regulatory region and two HREs possessing HIF-1α binding activity in the minimal promoter region of the Drp1 gene. We also demonstrated that Drp1 can alleviate hypoxia-induced PASMCs proliferation and apoptosis by mitochondrial fission, whose levels increase with hypoxia in pulmonary vascular remodeling. Collectively, the data suggested that HIF-1α mediated the activation of Drp1 under hypoxic conditions that resulted in the induction of the mitochondrial pathway of proliferation and apoptosis in PASMCs, via the modulation of the expression of PCNA and Caspase-3.

4.1 Limitations

We acknowledge that this study have some limitations. Firstly, in our experiment, Mdivi-1, a mitochondrial division inhibitor, was used for intervention the mitochondrial dynamics, however there was no intervention study on inhibition or overexpression of Drp1 protein. It is suggested that small RNA interference technology should be used for further study of Drp1 in subsequent experiments. Secondly, in this study, mitochondrial dynamics disorder has an important effect on the development of pulmonary hypertension, but the mechanism of mitochondrial fission related protein Drp1 affects the proliferation and apoptosis of pulmonary vascular smooth muscle cells has not been clarified. Therefore, further studies are required to examine the mechanism.

4.2 Conclusions

In conclusion, HIF-1α is overexpressed in hypoxia-in-

duced pulmonary vascular remodeling *in vivo* and *in vitro*. HIF-1α promoted PASMC cell proliferation and inhibited hypoxia-induced apoptosis, possibly through the regulation of mitochondrial dynamics via Drp1. Based on these findings, HIF-1α might serve as a useful biomarker and therapeutic target in PH. Moreover, this study provides the preliminary evidence for the therapeutic potential of the HIF-1α/Drp1 signaling pathway in the treatment of hypoxic pulmonary vascular remodeling.

Acknowledgments

This study was supported by the National Natural Science Foundation of China (No. 81673858, No. 81704062, No. 30500644), the Science and Technology Project of Traditional Chinese Medicine in Hunan (No. 2009045, No. 2012027), and the Program for National Center for Clinical Medicine for Geriatric Diseases (Ministry of Science and Technology). All authors had no conflicts of interest to disclose.

References

1 Hemnes AR, Humbert M. Pathobiology of pulmonary arterial hypertension: understanding the roads less travelled. *Eur Respir Rev* 2017; 26: 170093.
2 Paulin R, Meloche J, Courboulin A, *et al*. Targeting cell motility in pulmonary arterial hypertension. *Eur Respir J* 2014; 43: 531–544.
3 Khanam R, Kumar R, Hejazi II, *et al*. Piperazine clubbed with 2-azetidinone derivatives suppresses proliferation, migration and induces apoptosis in human cervical cancer HeLa cells through oxidative stress mediated intrinsic mitochondrial pathway. *Apoptosis* 2018; 23: 113–131.
4 Chan DC. Fusion and fission: interlinked processes critical for mitochondrial health. *Annu Rev Genet* 2012; 46: 265–287.
5 Zhao J, Lendahl U, Nistér M. Regulation of mitochondrial dynamics: convergences and divergences between yeast and vertebrates. *Cell Mol Life Sci* 2013; 70: 951–976.
6 Parra V, Bravo-Sagua R, Norambuena-Soto I, *et al*. Inhibition of mitochondrial fission prevents hypoxia-induced metabolic shift and cellular proliferation of pulmonary arterial smooth muscle cells. *Biochim Biophys Acta Mol Basis Dis* 2017; 1863: 2891–2903.
7 Boehme J, Sun X, Tormos KV, *et al*. Pulmonary artery smooth muscle cell hyperproliferation and metabolic shift triggered by pulmonary overcirculation. *Am J Physiol Heart Circ Physiol* 2016; 311: H944–H957.
8 Archer SL. Acquired mitochondrial abnormalities, including epigenetic inhibition of superoxide dismutase 2, in pulmonary hypertension and cancer: therapeutic implications. *Adv Exp Med Biol* 2016; 903: 29–53.
9 Shimoda LA, Manalo DJ, Sham JS, *et al*. Partial HIF-1alpha deficiency impairs pulmonary arterial myocyte electrophysiological responses to hypoxia. *Am J Physiol Lung Cell Mol Physiol* 2001; 281: L202–L208.
10 Dessouroux A, Akwa Y, Baulieu EE. DHEA decreases HIF-1alpha accumulation under hypoxia in human pulmonary artery cells: potential role in the treatment of pulmonary arterial hypertension. *J Steroid Biochem Mol Biol* 2008; 109: 81–89.
11 Irwin DC, McCord JM, Nozik-Grayck E, *et al*. A potential role for reactive oxygen species and the HIF-1alpha-VEGF pathway in hypoxia-induced pulmonary vascular leak. *Free Radic Biol Med* 2009; 47: 55–61.
12 Semba H, Takeda N, Isagawa T, *et al*. HIF-1alpha-PDK1 axis-induced active glycolysis plays an essential role in macrophage migratory capacity. *Nat Commun* 2016; 7: 11635.
13 Bernard O, Jeny F, Uzunhan Y, *et al*. Mesenchymal stem cells reduce hypoxia-induced apoptosis in alveolar epithelial cells by modulating HIF and ROS hypoxic signaling. *Am J Physiol Lung Cell Mol Physiol* 2018; 314: L360–L371.
14 Wu Y, Meitzler JL, Antony S, *et al*. Dual oxidase 2 and pancreatic adenocarcinoma: IFN-gamma-mediated dual oxidase 2 overexpression results in H2O2-induced, ERK-associated up-regulation of HIF-1alpha and VEGF-A. *Oncotarget* 2016; 7: 68412–68433.
15 Wang T, Zhang ZX, Xu YJ, *et al*. 5-Hydroxydecanoate inhibits proliferation of hypoxic human pulmonary artery smooth muscle cells by blocking mitochondrial K (ATP) channels. *Acta Pharmacol Sin* 2007; 28: 1531–1540.
16 Lu Y, Huang J, Geng S, *et al*. MitoKATP regulating HIF/miR210/ISCU signaling axis and formation of a positive feedback loop in chronic hypoxia-induced PAH rat model. *Exp Ther Med* 2017; 13: 1697–1701.
17 Li Q, Mao M, Qiu Y, *et al*. Key role of ROS in the process of 15-lipoxygenase/15-hydroxyeicosatetraenoiccid-induced pulmonary vascular remodeling in hypoxia pulmonary hypertension. *PLoS One* 2016; 11: e0149164.
18 Marsboom G, Toth PT, Ryan JJ, *et al*. Dynamin-related protein 1-mediated mitochondrial mitotic fission permits hyperproliferation of vascular smooth muscle cells and offers a novel therapeutic target in pulmonary hypertension. *Circ Res* 2012; 110: 1484–1497.
19 Bonnet S, Michelakis ED, Porter CJ, *et al*. An abnormal mitochondrial- hypoxia inducible factor-1alpha-Kv channel pathway disrupts oxygen sensing and triggers pulmonary arterial hypertension in fawn hooded rats: similarities to human pulmonary arterial hypertension. *Circulation* 2006; 113: 2630–2641.
20 Archer SL, Gomberg-Maitland M, Maitland ML, *et al*. Mitochondrial metabolism, redox signaling, and fusion: a mitochondria-ROS-HIF-1alpha-Kv1.5 O2-sensing pathway at the intersection of pulmonary hypertension and cancer. *Am J Physiol Heart Circ Physiol* 2008; 294: H570–H578.
21 Gao Z, Li Y, Wang F, *et al*. Mitochondrial dynamics controls

anti-tumour innate immunity by regulating CHIP-IRF1 axis stability. *Nat Commun* 2017; 8: 1805.
22 Fang X, Chen X, Zhong G, *et al*. Mitofusin 2 downregulation triggers pulmonary artery smooth muscle cell proliferation and apoptosis imbalance in rats with hypoxic pulmonary hypertension via the PI3K/Akt and mitochondrial apoptosis pathways. *J Cardiovasc Pharmacol* 2016; 67: 164–174.
23 Zhang WF, Zhu TT, Xiong YW, *et al*. Negative feedback regulation between microRNA let-7g and LOX-1 mediated hypoxia-induced PASMCs proliferation. *Biochem Biophys Res Commun* 2017; 488: 655–663.
24 Zhu TT, Zhang WF, Luo P, *et al*. Epigallocatechin-3-gallate ameliorates hypoxia-induced pulmonary vascular remodeling by promoting mitofusin-2-mediated mitochondrial fusion. *Eur J Pharmacol* 2017; 809: 42–51.
25 Li YX, Run L, Shi T, *et al*. CTRP9 regulates hypoxia-mediated human pulmonary artery smooth muscle cell proliferation, apoptosis and migration via TGF-β1/ERK1/2 signaling pathway. *Biochem Biophys Res Commun* 2017; 490: 1319–1325.
26 Wang AP, Li XH, Gong SX, *et al*. miR-100 suppresses mTOR signaling in hypoxia-induced pulmonary hypertension in rats. *Eur J Pharmacol* 2015; 765: 565–573.
27 Xia Y, Chen Z, Chen A, *et al*. LCZ696 improves cardiac function via alleviating Drp1-mediated mitochondrial dysfunction in mice with doxorubicin-induced dilated cardiomyopathy. *J Mol Cell Cardiol* 2017; 108: 138–148.
28 Kumfu S, Chattipakorn S, Fucharoen S, *et al*. Mitochondrial calcium uniporter blocker prevents cardiac mitochondrial dysfunction induced by iron overload in thalassemic mice. *Biometals* 2012; 25: 1167–1175.
29 Thummasorn S, Kumfu S, Chattipakorn S, *et al*. Granulocyte-colony stimulating factor attenuates mitochondrial dysfunction induced by oxidative stress in cardiac mitochondria. *Mitochondrion* 2011; 11: 457–466.
30 Yu AY, Shimoda LA, Iyer NV, *et al*. Impaired physiological responses to chronic hypoxia in mice partially deficient for hypoxia-inducible factor 1alpha. *J Clin Invest* 1999; 103: 691–696.
31 Ball MK, Waypa GB, Mungai PT, *et al*. Regulation of hypoxia-induced pulmonary hypertension by vascular smooth muscle hypoxia-inducible factor-1alpha. *Am J Respir Crit Care Med* 2014; 189: 314–324.
32 Shan F, Li J, Huang QY. HIF-1 alpha-induced up-regulation of miR-9 contributes to phenotypic modulation in pulmonary artery smooth muscle cells during hypoxia. *J Cell Physiol* 2014; 229: 1511–1520.
33 Chettimada S, Gupte R, Rawat D, *et al*. Hypoxia-induced glucose-6-phosphate dehydrogenase overexpression and -activation in pulmonary artery smooth muscle cells: implication in pulmonary hypertension. *Am J Physiol Lung Cell Mol Physiol* 2015; 308: L287–L300.
34 Tuder RM, Chacon M, Alger L, *et al*. Expression of angiogenesis-related molecules in plexiform lesions in severe pulmonary hypertension: evidence for a process of disordered angiogenesis. *J Pathol* 2001; 195: 367–374.
35 Fijalkowska I, Xu W, Comhair SA, *et al*. Hypoxia inducible-factor1alpha regulates the metabolic shift of pulmonary hypertensive endothelial cells. *Am J Pathol* 2010; 176: 1130–1138.
36 Han CF, Li ZY, Li TH. Roles of hypoxia-inducible factor-1α and its target genes in neonatal hypoxic pulmonary hypertension. *Eur Rev Med Pharmacol Sci* 2017; 21: 4167–4180.
37 Archer SL. Mitochondrial dynamics--mitochondrial fission and fusion in human diseases. *N Engl J Med* 2013; 369: 2236–2251.
38 Ruan L, Zhou C, Jin E, *et al*. Cytosolic proteostasis through importing of misfolded proteins into mitochondria. *Nature* 2017; 543: 443–446.
39 Senyilmaz D, Virtue S, Xu X, *et al*. Regulation of mitochondrial morphology and function by stearoylation of TFR1. *Nature* 2015; 525: 124–128.
40 Franco A, Kitsis RN, Fleischer JA, *et al*. Correcting mitochondrial fusion by manipulating mitofusin conformations. *Nature* 2016; 540: 74–79.
41 Barnes EA, Chen CH, Sedan O, *et al*. Loss of smooth muscle cell hypoxia inducible factor-1alpha underlies increased vascular contractility in pulmonary hypertension. *FASEB J* 2017; 31: 650–662.
42 Wang Y, Subramanian M, Yurdagul A Jr, *et al*. Mitochondrial fission promotes the continued clearance of apoptotic cells by macrophages. *Cell* 2017; 171: 331–345.
43 Frezza C, Cipolat S, Martins de Brito O, *et al*. OPA1 controls apoptotic cristae remodeling independently from mitochondrial fusion. *Cell* 2006; 126: 177–189.
44 Shen T, Wang N, Yu X, *et al*. The critical role of dynamin-related protein 1 in hypoxia-induced pulmonary vascular angiogenesis. *J Cell Biochem* 2015; 116: 1993–2007.
45 Zhang L, Ma C, Zhang C, *et al*. Reactive oxygen species effect PASMCs apoptosis via regulation of dynamin-related protein 1 in hypoxic pulmonary hypertension. *Histochem Cell Biol* 2016; 146: 71–84.
46 Cho B, Cho HM, Jo Y, *et al*. Constriction of the mitochondrial inner compartment is a priming event for mitochondrial division. *Nat Commun* 2017; 8: 15754.
47 Uo T, Dworzak J, Kinoshita C, *et al*. Drp1 levels constitutively regulate mitochondrial dynamics and cell survival in cortical neurons. *Exp Neurol* 2009; 218: 274–285.